JOURNAL OF MATERIALS SCIENCE 28 (1993) 145–154

Acoustic emission during tensile deformation of annealed and cold-worked AISI type 304 austenitic stainless steel

C. K. MUKHOPADHYAY, K. V. KASIVISWANATHAN, T. JAYAKUMAR, BALDEV RAJ
Division for PIE and NDT Development, Indira Gandhi Centre for Atomic Research, Kalpakkam 603 102, India

The influence of prior cold work on the acoustic emission (AE) generated during subsequent plastic deformation of AISI type 304 stainless steel has been studied. AE parameters such as root mean square voltage, ringdown counts, etc., have been used to analyse the data. AE generated during tensile deformation is affected by prior cold work. The increase in acoustic activity at low strain levels in a less cold-worked (10%) specimen compared to a solution-annealed specimen was attributed to the easy formation of α'-martensite assisted by prior cold work. The decreased acoustic activity for higher cold-worked (20%, 40% and 50%) specimens at low strain levels was attributed to reduced glide distance for moving dislocations and reduced amount of α'-martensite formation. The AE activity was found to be maximum during higher strain values in the solution-annealed specimen compared to the cold-worked specimens. This was attributed to relatively larger amount of α'-martensite formation in the solution-annealed specimen. Eddy current testing, X-ray diffraction, remanent magnetization measurement and magnetic etching techniques have been used to corroborate the AE results. Among these, remanent magnetization results were found to have good correlation with the AE results.

1. Introduction

AISI type 304 stainless steel undergoes strain-induced transformation ($\gamma \rightarrow \alpha'$) when plastically deformed under uniaxial tension at ambient temperature [1–3]. The crystallography of this transformation and its response to the variations of strain, strain rate and temperature are fairly well established [4, 5]. It has also been reported that transformation in AISI 304 stainless steel is strain-induced rather than stress-assisted [2, 3]. In this type of transformation, nucleation sites are created during plastic deformation. Deformation of the parent phase (γ) creates the proper defect structure which acts as an embryo for the transformation phase (α'). The unstable austenite first transforms into hexagonal close-packed (h c p) ε-martensite by the movement of partial dislocations on the (1 1 1) planes of the metastable austenite matrix. Subsequently, the band originally built of stacking faults is transformed to α'-martensite [6]. The internal structure of α'-martensite is characterized by high dislocation density rather than by twins.

The kinetics of the strain-induced $\gamma \rightarrow \alpha'$ transformation have been theoretically modelled [7] and the theoretical results have been found to agree fairly well with the results obtained by magnetic techniques used to monitor the progress of the $\gamma \rightarrow \alpha'$ transformation in AISI 304 stainless steel [8].

The prior low-temperature plastic deformation (i.e. cold work) of the parent phase (γ) influences the subsequent nucleation and growth of martensite during tensile deformation in strain-assisted transformation. Nucleation is assisted by small amounts of plastic deformation, while extensive cold working suppresses nucleation [9–11]. The present investigations were planned to study the influence of prior cold work on the strain-induced martensitic transformation during tensile deformation in AISI 304 stainless steel using acoustic emission technique (AET). AET was used because it has the unique potential to monitor the phase transformation on-line. Acoustic emission (AE) occurs during tensile deformation due to transient rapid release of energy from localized sources, such as regions of relaxation of stress and strain fields. AE generated during tensile deformation strongly depends on the microstructural features, deformation processes and phase transformations [12–18]. AE parameters such as root mean square (r.m.s) voltage, ringdown counts, etc., have been used to characterize the tensile deformation process in the annealed and cold-worked AISI 304 stainless steel. Various techniques, such as eddy current testing, X-ray diffraction, magnetic remanence measurement and magnetic etching, have been used to identify and quantify $\gamma \rightarrow \alpha'$ transformation during

0022–2461

cold work and subsequent tensile deformation. The results from these techniques have been used to corroborate the AE results.

2. Experimental procedure

The material used in the present investigation was AISI type 304 austenitic stainless steel having the following chemical composition (wt %) : 0.08 C, 18.0 Cr, 10.5 Ni, 2.0 Mn, 1.0 Si, 0.002 S, 0.03 P and balance Fe. Flat sheet tensile specimens having gauge dimensions 36 mm × 8 mm × 5 mm were prepared from plates in solution-annealed (1323 K, 1 h) as well as in four different cold-worked conditions (10%, 20%, 40% and 50%). All the specimens were polished with 400 grit emery paper to obtain a uniform surface finish. Tensile testing was carried out at a nominal strain rate of $5 \times 10^{-4} s^{-1}$ at ambient temperature (~298 K). AE signals generated during tensile deformation were recorded and analysed using an AET-5000 system. A piezoelectric transducer (8 mm diameter) having resonant frequency at 175 kHz, a preamplifier (60 dB gain) and a compatible filter (125–250 kHz) were used to capture the signal. The transducer was fixed at the gauge to shoulder transition regions of the tensile specimens. Fig. 1 shows a schematic drawing of the experimental apparatus. A total system gain of 90 dB and a threshold of 0.9 V were maintained throughout the experiment. The gain and threshold were so selected that no external noise was picked up. This was verified by repeatedly loading and unloading a dummy specimen to more than 1.5 times the maximum load expected to be taken by any of the specimens used in this study. Except during the first cycle of loading, no emission was generated during subsequent loading, indicating that AE signals were not recorded from the machine and external noise. Characterization of α'-martensite phase was carried out using X-ray diffraction and electro-magnetic methods.

X-ray diffraction measurements were made using a Siemens D500 model powder diffractometer using a diffracted beam monochromator (graphite) on small samples cut from the shoulder and fracture regions of the tensile-tested specimens, in order to detect the α' (b c c) phase formed as a result of strain-induced martensitic transformation. The samples taken from the shoulder regions show the α' phase formed by cold work alone and the samples taken from fracture regions show the α' formed after cold work and subsequent tensile testing. Diffraction patterns were taken at a scanning speed of 2° min^{-1} using CuK_α radiation. During recording, the samples were rotated on their own plane at 30 r.p.m.

Remanent magnetization (or remanence) of various specimens were measured in the as-cold-worked and cold-worked and tensile-tested conditions. For this, longitudinal samples were cut 5 mm away from the fracture surfaces of the tensile-tested specimens. The samples were demagnetized by passing them through a d.c. field with the longitudinal axis perpendicular to the field, and then magnetized in the same direction. Remanence was measured on both sides of the samples by using a gaussmeter.

Samples used for magnetic etching were prepared by cutting, mounting and polishing of small portions from the shoulder and near the fracture regions. Magnetic etching was done with the help of a magnetic solution of colloidal particles to see the morphology and distribution of the magnetic phase (α'-martensite)

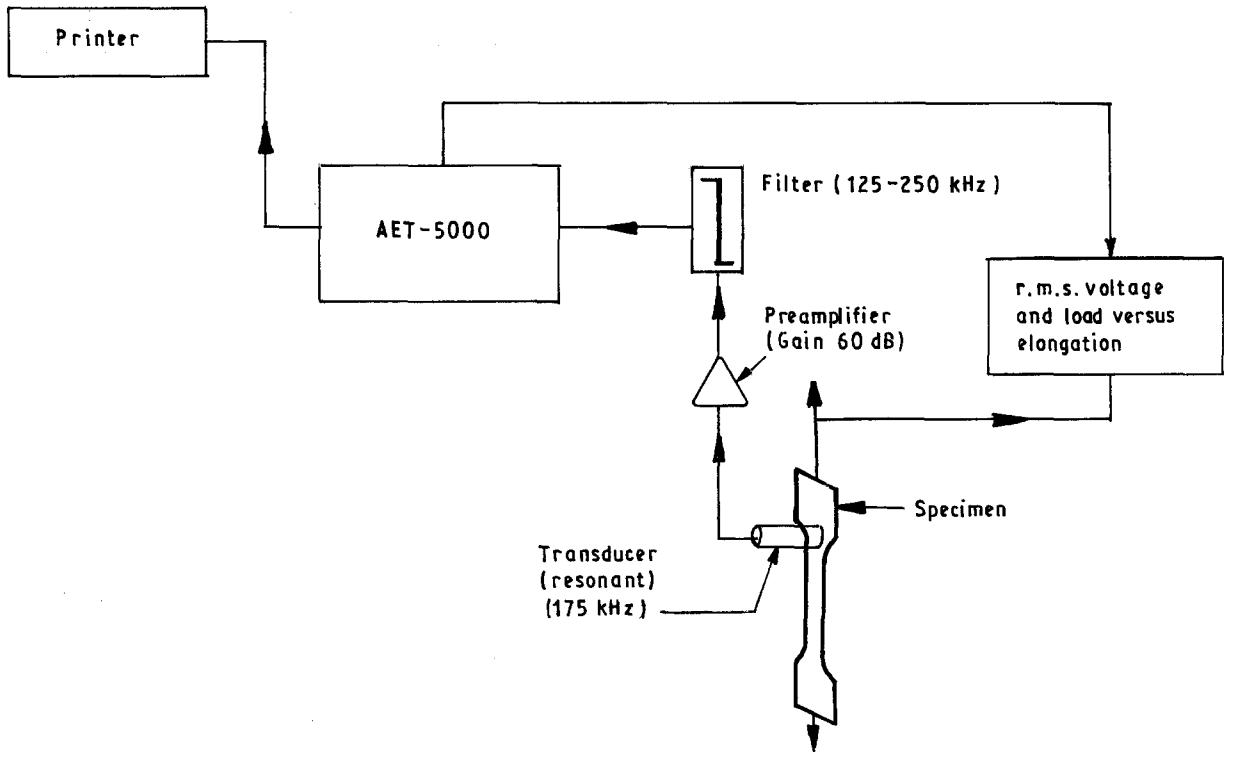

Figure 1 Schematic drawing of experimental apparatus.

in the specimens. For this, a magnetic solution was applied to the polished samples and observed microscopically. A cover slip was used to prevent evaporation of the fluid and the magnetic particles were allowed to settle for some time on the polished surfaces. The pattern of the settled particles was photographed with the magnetic field in "off" and "on" conditions. In the "off" condition, the particles were settled randomly as these were not affected by any magnetic field. In the "on" condition, the settled particles were attracted towards the magnetic phase present on the steel samples under the influence of the magnetic field. This enabled observation of the preferential attraction of the colloidal magnetic particles towards the magnetic phase present on the polished surfaces of the stainless steel samples in the "on" condition.

3. Results and discussion

3.1. Tensile properties

Table I gives the tensile properties of the specimens. The values are the average of at least two measurements. Increase in the strength and decrease in the ductility are observed with increase in the prior cold work.

3.2. Acoustic emission

Fig. 2 shows the engineering stress–strain curves for the specimens with different degrees of cold work. The curves showing the variation in r.m.s. voltage of AE signal with strain are also superimposed on to the stress–strain plots. Variation in AE ringdown counts with strain for different specimens is shown in Fig. 3. The arrows shown in the plots indicate 0.2% offset yield strength (YS). Events also showed similar trends, such as ringdown counts. Intense AE is generated up to low strain values in the solution-annealed specimen, which is attributed to dislocation avalanche by dislocation generation and multiplication by operation of Frank–Read (FR) and grain-boundary (GB) sources and dislocation motion during yielding [19]. Both ringdown counts and r.m.s. voltage indicate that the acoustic activity generated up to low strain levels increases for 10% and then decreases again for higher (20%, 40% and 50%) cold-worked specimens, compared to annealed specimens. The reduced emission for higher cold-worked specimens could be attributed to the decreased glide distance for moving dislocations by prior cold work, in accordance with the model proposed by Agarwal *et al.* [20]. By the same explanation, the AE activity in the 10% cold-worked specimen should also be lower in comparison to the solution-annealed specimen. However, the highest AE activity in 10% cold-worked specimen is explained as follows: as mentioned above, small amounts of prior cold work assist in α'-martensite formation during subsequent transformation [9–11]. It is also known that the formation of α' from γ takes place through formation of ε. So, the prior cold work first transforms the γ to ε thus creating the nucleation sites for α' [21, 22]. The observed higher AE activity in the 10% cold-worked specimen is therefore attributed to easy formation of α'-martensite from the ε-martensite that formed during prior cold work. On the other hand, with increase in prior cold work, nucleation of α'-martensite is suppressed [9–11]. This also should have contributed to the reduced AE activity in higher cold-worked specimens, in addition to the reduced glide distance already mentioned.

It is also seen from Figs 2 and 3 that considerable AE is generated in the region of progressive plastic deformation in the solution-annealed specimen. On the other hand, AE studies during tensile deformation of annealed 316 stainless steel has shown that the AE activity in post-yield region is very small [19]. Because the AISI type 316 stainless steel with more stable austenite does not show the phenomenon of strain-induced martensitic transformation at ambient temperature, the reduced post-yield AE activity has been attributed to the decrease in both glide distance for moving dislocations, and the rate of formation of dislocation avalanche. Therefore, the presence of higher acoustic activity in the post-yield uniform deformation region of the present material could be attributed to the phenomenon of strain-induced martensitic transformation. This is also supported by the fact that a minimum amount of strain is needed for the strain–induced martensite formation to take place. It may be noted that the strain axis in Fig. 2 has been expanded for the cold worked specimens. It can be seen from Fig. 2 that the amount of post-yield deformation (beyond the arrow indicated in Fig. 2) is reduced in higher cold-worked specimens. Because most of the α' martensite formation is expected during prior cold work and up to the yield region during subsequent tensile loading in cold-worked specimens, only small amounts of α' are expected to form during the post-yield region leading to reduced AE activity. It is also known that the rate of martensite formation upon straining a metastable austenitic steel depends

TABLE I Tensile properties of AISI Type 304 stainless steel

Cold work (%)	0.2% offset yield strength (MPa)	Ultimate tensile strength (MPa)	Total elongation (%)	Uniform elongation (%)
0	183	551	72.2	66.1
10	461	612	60.0	52.8
20	667	750	25.0	16.4
40	777	915	16.1	12.2
50	965	1007	9.1	5.2

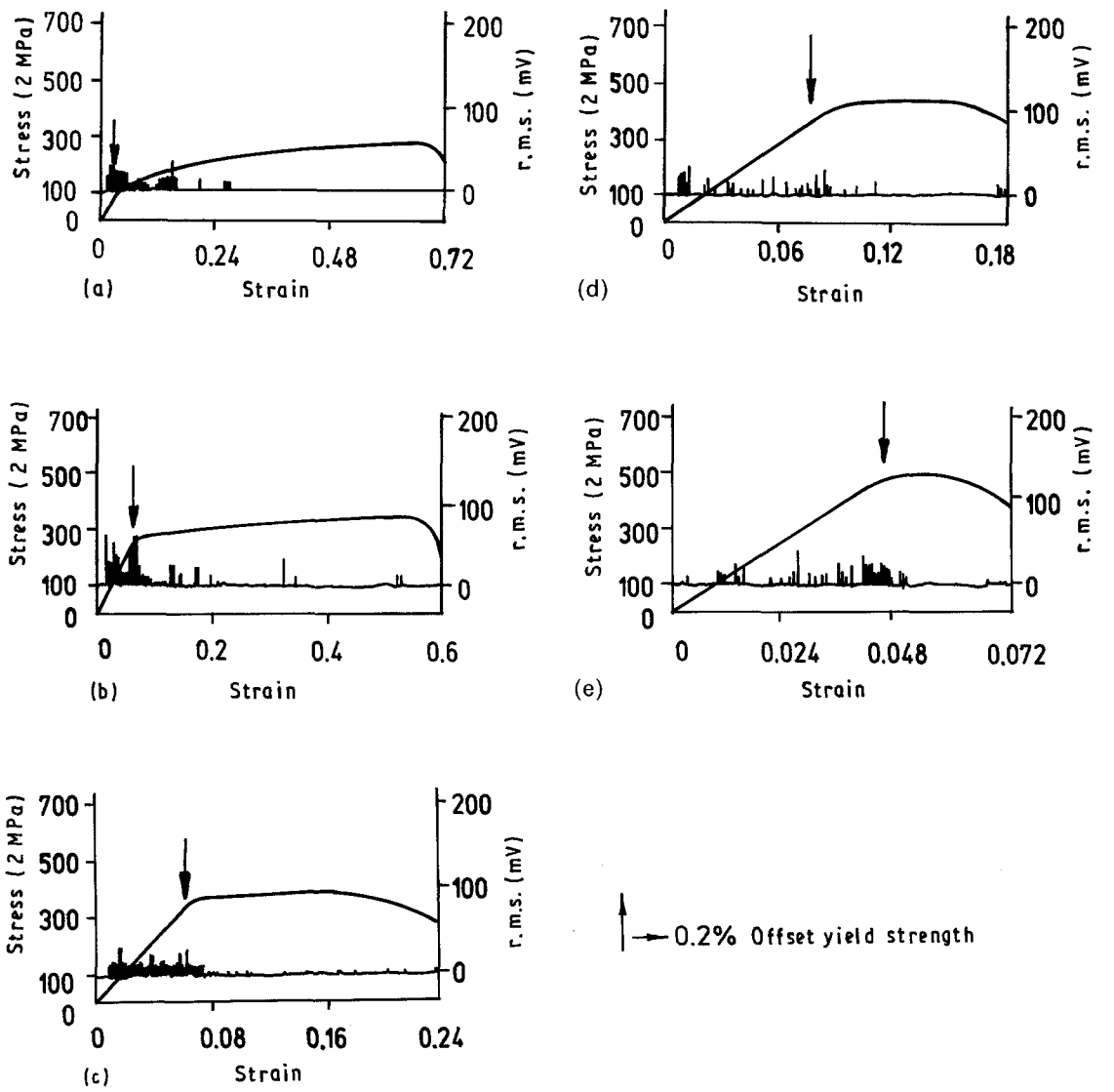

Figure 2 Engineering stress and root mean square (r.m.s.) voltage of AE signal versus engineering strain plots for AISI type 304 stainless steel. (a) Annealed; and cold worked (b) 10%, (c) 20%, (d) 40%, (e) 50%.

on the stability of austenite. For a given deformation temperature, the austenite stability is a function of the alloy content and the thermomechanical history. Large amounts of deformation of austenite increase its dislocation density and thus make the cooperative movement of atoms required for the formation of martensite more difficult [23]. This explains the formation of the reduced amount of α′-martensite during tensile deformation with correspondingly lower AE activity in the higher cold-worked specimens.

Peak amplitude distribution of the events generated up to a strain corresponding to YS for annealed and 10% cold-worked specimens is shown in Fig. 4. Many higher peak amplitude (PA) events seen in the 10% cold-worked specimen are attributed to the strain-induced martensitic transformation.

Fig. 5 shows the logarithmic cumulative amplitude distribution plots of the AE events obtained during the complete tensile tests of annealed and different cold-worked specimens. Amplitude distribution analysis is a useful way of characterizing the AE signal and can yield information that is not obtainable by other parameters [24]. Amplitude of the AE signal is related to the energy of the source. Therefore, it is logical to employ amplitude distribution analysis to characterize the source of AE. The distribution of peak amplitude values is carried out by the measurement of the peak amplitudes of the individual events. Amplitude distribution detected by a resonant transducer is characterized by the following equation [25].

$$F(V) = (V/V_0)^{-b} \quad (1)$$

where V is the instantaneous voltage, $F(V)$ is the number of the AE events having amplitude greater than V, and V_0 is the lowest detectable amplitude. b is the slope of the log–log plot of $F(V)$ versus V. This slope is termed the b-parameter and characterizes the source strength. Thus, it becomes very convenient to describe the whole distribution by specifying a single parameter b. A higher value of b indicates a signal having a large number of small-amplitude events, whereas a lower b value signifies a signal consisting of an increased number of high-amplitude signals. The b parameters for different specimens, based on the procedure given above, have been computed from the plots shown in Fig. 5. The variation in b with degree of cold work is shown in Fig. 6. It can be seen from Fig. 6

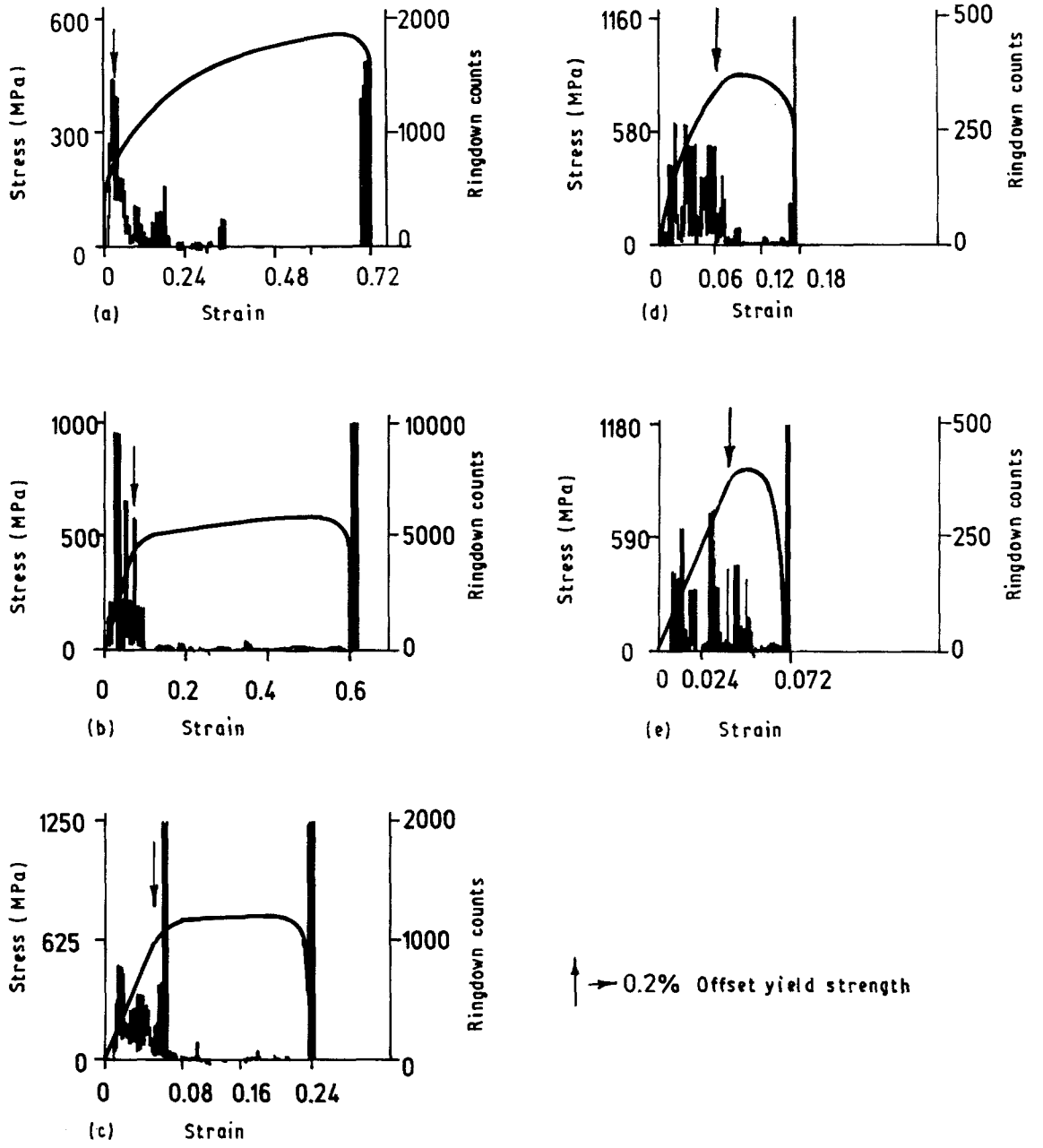

Figure 3 Engineering stress and AE ringdown counts versus engineering strain plots for AISI type 304 stainless steel. (a) Annealed; and cold-worked (b) 10%, (c) 20%, (d) 40%, (e) 50%.

that the value of b decreases for the 10% cold-worked specimen compared to the solution-annealed specimen but increases again for 20%, 40% and 50% cold-worked specimens. The lower value of b in the case of the 10% cold-worked specimen is attributed to the dominance of higher amplitude events associated with the greater amount of α′-martensite transformation. A gradually reduced amount of α′-martensite is formed during tensile deformation in 20%, 40% and 50% cold-worked specimens due to a reduction in this transformation, as discussed earlier. The few higher PA events associated with this transformation cannot be reflected in the amplitude distribution plot, and therefore results in a higher b-parameter for 20%, 40% and 50% cold-worked specimens, compared to the 10% cold-worked specimen.

3.3. Eddy current testing

Results of earlier work relating to eddy current measurements using surface probe (EM 3300 Multitest Automation Sperry, USA) on the cold-worked specimens of the same material [26] are shown in Fig. 7. It can be seen that considerable increase in eddy current output, representing the increased amount of magnetic phase, has been obtained for the specimens with cold work beyond 10%. This implies that an almost negligible amount of magnetic phase is formed below 10% cold work.

3.4. X-ray diffraction

Fig. 8 shows the results obtained for the annealed specimen in the pre- and post-tensile-tested conditions. It can be seen from Fig. 8 that peaks of $(1\,1\,1)_{\gamma'}$ $(2\,0\,0)_{\gamma}$ and $(2\,2\,0)_{\gamma}$ are present in the diffraction trace of the annealed specimen before tensile testing. The appearance of a new peak identified as $(1\,1\,0)_{\alpha'}$ after tensile testing in the diffraction trace of the annealed

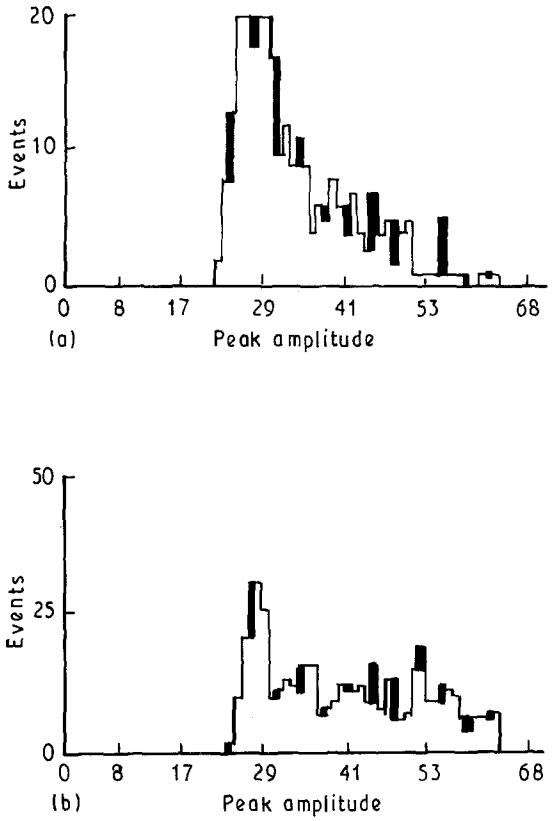

Figure 4 Peak amplitude distribution of events (up to yielding) for (a) annealed and (b) 10% cold-worked AISI type 304 stainless steel.

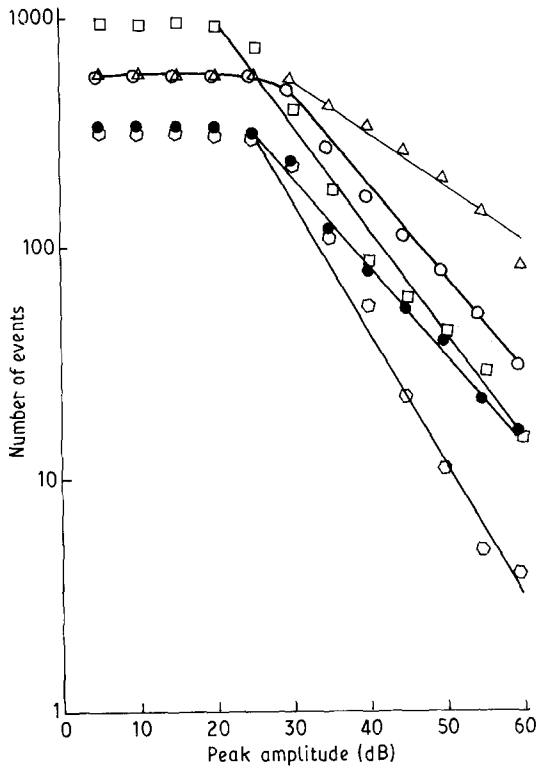

Figure 5 Logarithmic cumulative amplitude distribution plots of the AE signal obtained during tensile testing of AISI type 304 stainless steel. (○) Annealed; cold-worked (△) 10%, (□) 20%, (●) 40%, ( ) 50%.

specimen is clear evidence for the strain-induced martensitic transformation during uniaxial tensile deformation. X-ray diffraction traces for the cold-worked specimens were not included in this plot

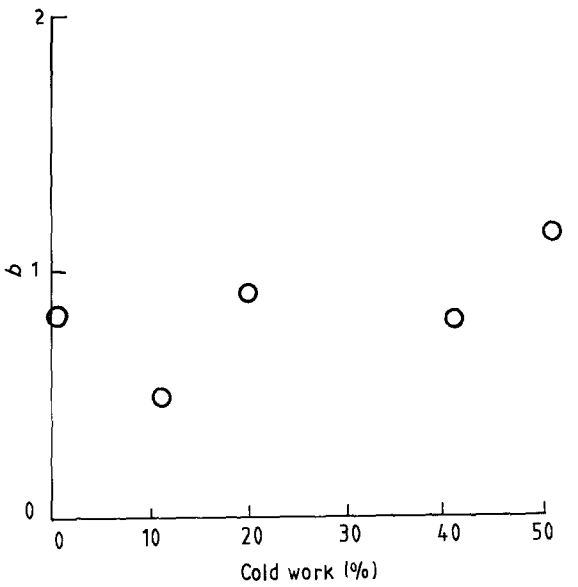

Figure 6 Variation of b-parameters of AE signal with per cent prior cold work for AISI type 304 stainless steel.

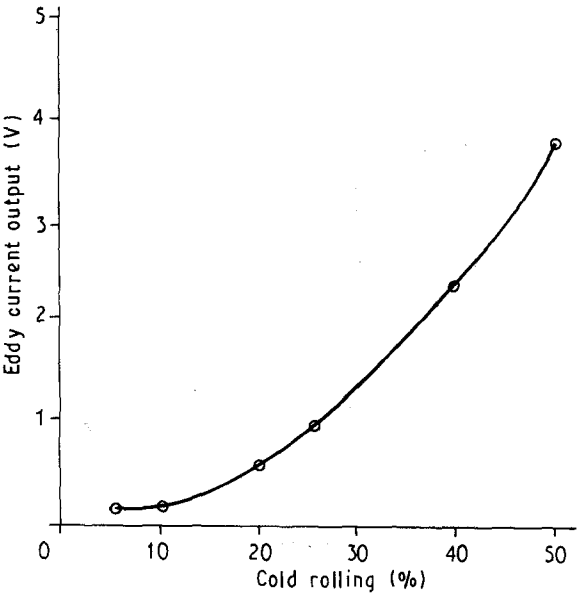

Figure 7 Eddy current output versus per cent cold rolling for AISI type 304 stainless steel at 200 kHz.

because of the inconsistency of the peak intensity values of the austenite and martensite lines obtained. This inconsistency is attributed to the presence of texture. However, the existence of bcc α' phase was indicated in various specimens in the as-cold-worked, cold-worked and tensile-tested conditions.

3.5. Remanence measurements and magnetic etching

AE results obtained during the present investigation have also been supported by the magnetic techniques. Because martensite (α') is ferromagnetic while austenite is paramagnetic, the existence of magnetic phase in the deformed specimens could evidently be used to provide support for strain-induced martensitic transformation. Two kinds of magnetic technique, namely

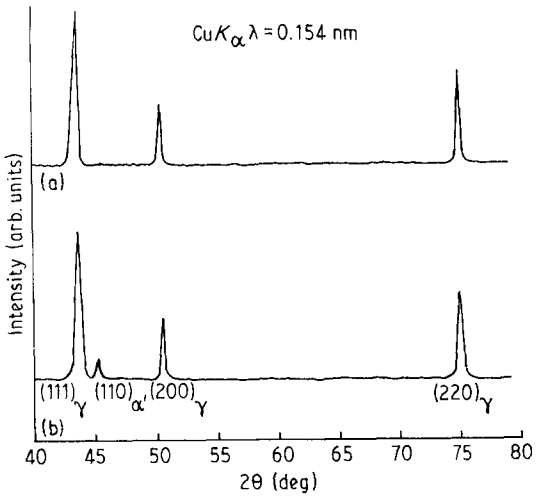

Figure 8 X-ray diffractometer traces of (a) as-annealed, and (b) annealed and tensile-tested AISI type 304 stainless steel.

(i) remanence measurements and (ii) revealing of magnetic phase by magnetic etching, were employed in this study.

It has been demonstrated that remanence measurements can be used to evaluate the strain-induced martensite (α′) phase in AISI 304 stainless steel [27]. The results obtained from the measurement of remanence in the as-cold-worked, cold-worked and tensile-tested conditions (Fig. 9a) and the difference in the remanence between the two conditions (Fig. 9b) are plotted as a function of prior cold work (Fig. 9). Remanence measurements made on 5% and 15% cold-worked specimens obtained from a separate study but on the same material [26], are also included in this plot. It is seen from this plot that, the difference in remanence between the two conditions increases up to a value of 10%–15% cold work and thereafter decreases at higher cold work. Therefore, increase in the difference in remanence values between the two conditions at the 10% cold-work level also confirms the earlier argument that a greater amount of strain-induced α′-martensite is formed in the 10% cold-worked specimen with a correspondingly higher acoustic activity during tensile deformation. The gradual decrease in the difference in remanence with increased prior cold work shows the reduction, of this transformation in the higher cold-worked specimens.

Magnetic etching also revealed the presence of α′-martensite in different specimens in the as-cold-worked, cold-worked and tensile-tested conditions. Results of magnetic etching of annealed and 50% cold-worked specimens are included and shown in Fig. 10a–d and e–h respectively. It can be seen that, in the magnetic field "off" condition, the colloidal magnetic particles are aligned randomly. In the "on" condition, the particles are attracted towards the magnetic phase present in the steel samples, resulting in the coalescence of the magnetic particles. Examples of these can be seen as circled regions in Fig. 10a and b. No comparison of the quantity of magnetic phase between the different specimens is possible because of the random settlement of the colloidal particles during the magnetic field "off" condition.

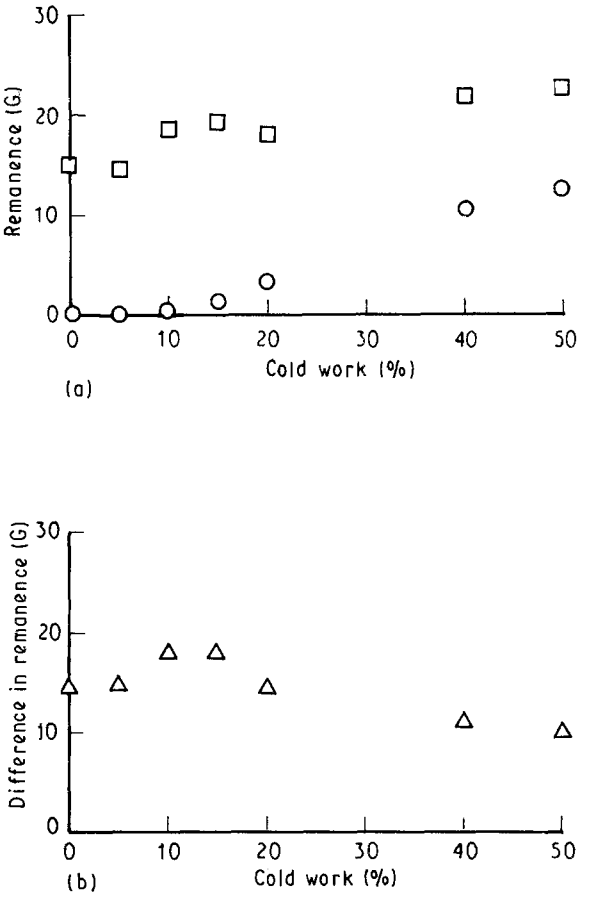

Figure 9 Variation of (a) remanent magnetization or (b) difference in remanence (between cold worked and tensile tested and as-cold-worked conditions) with per cent prior cold work. Magnetization, 3000 G. (a) (□) Cold-worked and tensile-tested, (○) as-cold-worked.

It is seen that, amongst the various techniques used in this study, the magnetic remanence measurement was the most successful in supporting the explanations given for the observed dependence of AE activity on the martensite formation during tensile deformation in different specimens.

4. Conclusion

Acoustic emission generated during tensile deformation of annealed and cold-worked AISI 304 stainless steel has been studied. The decrease in acoustic activity at low strain levels with increase in prior cold work is attributed to the decreased glide distance for moving dislocations, with the exception of 10% cold work. The increased acoustic activity in the 10% cold-worked specimen at low strain levels is the results of easy formation of α′-martensite assisted by prior cold work. Decreased AE in the case of higher cold-worked specimens (20%, 40% and 50%) is also attributed to the reduced amount of strain-induced α′-martensite transformation in these specimens due to increased stability of austenite after higher amounts of prior cold work. At higher strain values, the AE activity is found to be maximum in the solution-annealed specimen, which is attributed to the higher amount of α′-martensite formation during tensile deformation, compared to

that in cold-worked specimens. Remanent magnetization emerged as the most successful technique for characterizing the magnetic phase and corroborating the AE results during the course of this investigation.

Acknowledgements

The authors thank Dr P. Rodriguez, Head, Metallurgy and Materials programme, for his keen interest and constant encouragement in this work. The

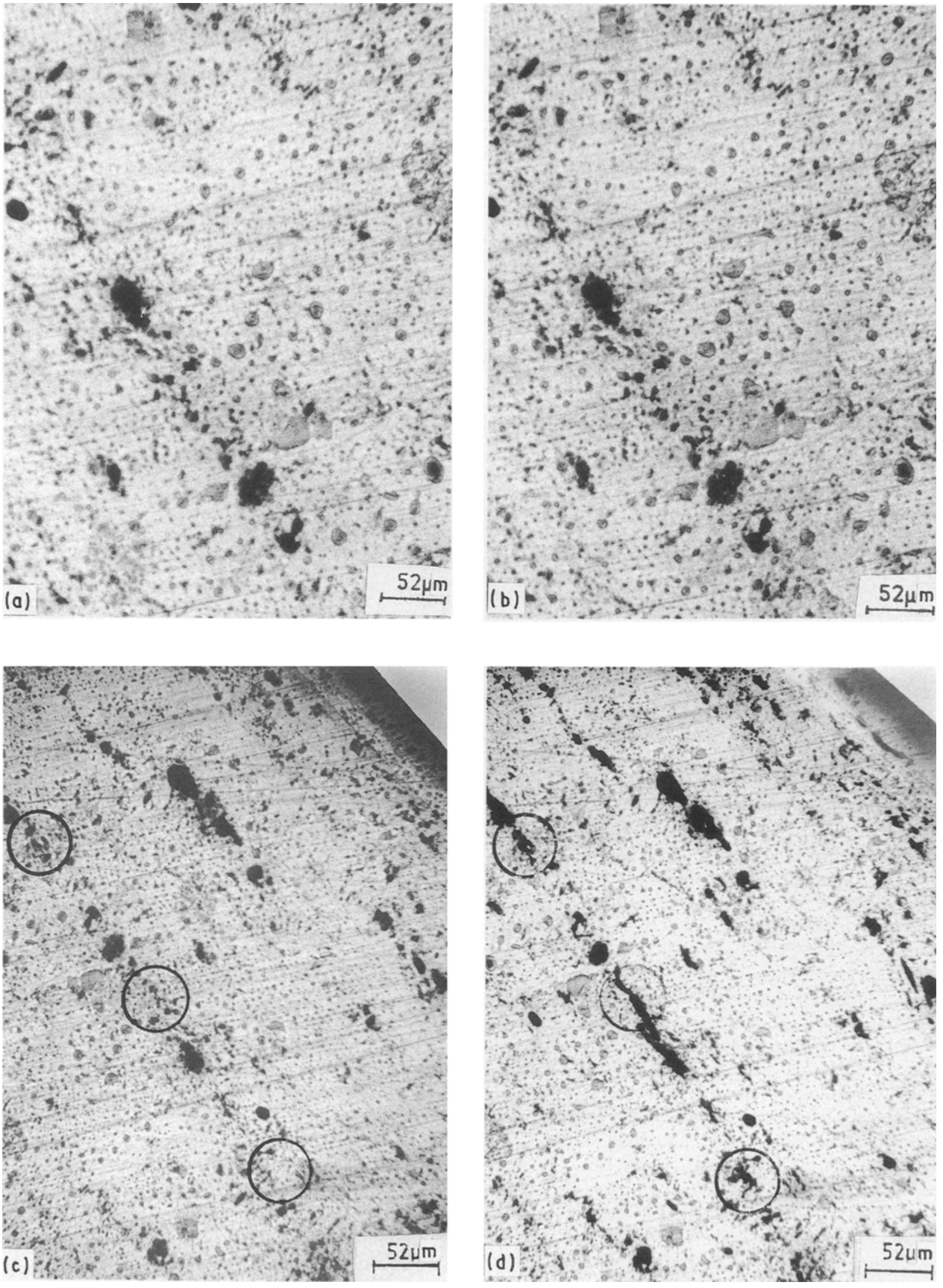

Figure 10 continued.

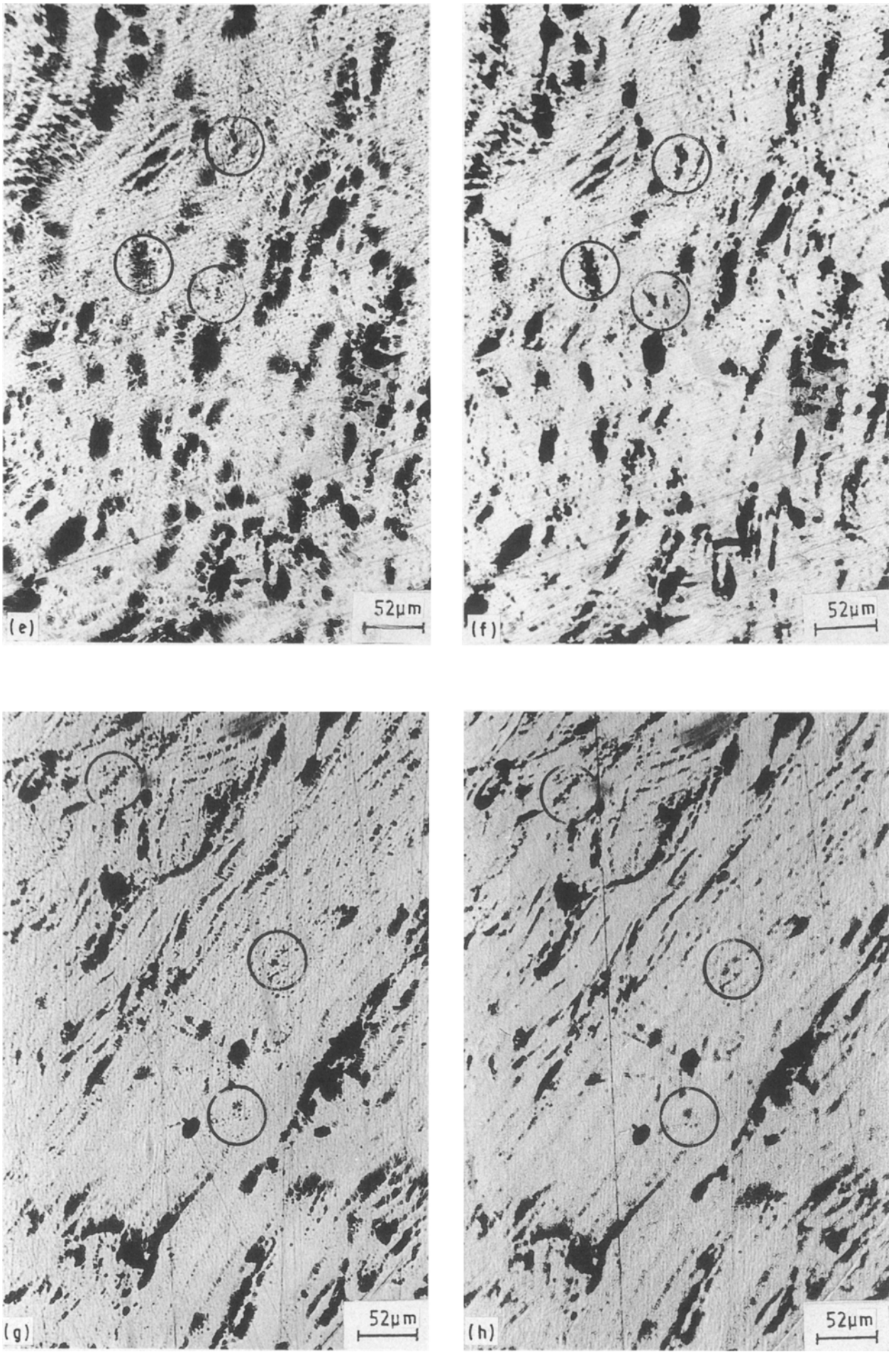

Figure 10 Magnetic colloidal suspension on (a, b) annealed, (c, d) annealed and tensile tested, and (e, f) 50% cold-worked and (g, h) 50% cold-worked and tensile tested AISI type 304 stainless steel. (a, c, e, g) Magnetic field "off". (b, d, f, h) Magnetic field "on".

authors also thank Dr. T. P. S. Gill and Mr S. Vaidyanathan for helping to carry out the magnetic etching and remanence measurement studies, respectively.

References

1. J. DASH and H. M. OTTE, *Acta Metall.* **11** (1963) 1169.
2. G. B. OLSON and M. COHEN, *J. Less-Common Metals* **28** (1972) 107.
3. P. C. MAXWELL, A. GOLDBERG and J. C. SHYNE, *Metall. Trans.* **5A** (1974) 1305.
4. R. LAGNEBORG, *Acta Metall.* **12** (1964) 823.
5. J. A. VENABLES, *Phil. Mag.* **7** (1962) 35.
6. U. REICHEL, B. GABRIEL, M. KESTEN, B. MEIER and W. DHAL, *Steel Res.* **60** (1989) 464.
7. G. B. OLSON and M. COHEN, *Metall. Trans.* **6A** (1975) 791.
8. S. S. HECKER, M. G. STOUT, K. P. STAUDHAMMER and J. L. SMITH, *ibid.* **13A** (1982) 619.
9. J. R. C. GUIMARAES and J. C. SHYNE, *Scripta Metall.* **4** (1970) 1019.
10. J. R. STRIFE, M. J. CARR and G. S. ANSELL, *Metall. Trans.* **8A** (1977) 1471.
11. J. F. BREEDIS, *Acta Metall.* **13** (1965) 2359.
12. BALDEV RAJ and T. JAYAKUMAR, in "Acoustic Emission: Current Practices and Future Directions", ASTM STP 1077 (American Society for Testing and Materials, Philadelphia, PA, 1990) pp. 218–41.
13. H. N. G. WADLEY, C. B. SCRUBY and J. H. SPAKE, *Int. Metals Rev.* **25** (1980) 41.
14. C. R. HEIPLE and S. H. CARPENTER, *J. Acoust. Emission* **6** (1987) 177.
15. *Idem., ibid.* **6** (1987) 215.
16. M. ITALANO, *J. Appl. Phys.* **48** (1977) 4397.
17. D. TSENG, Q. Y. LONG and K. TANGRI, *Acta Metall.* **35** (1987) 1887.
18. JAMES MOHR and AMIYA K. MUKHERJEE, *J. Acoust. Emission* **5** (1986) 162.
19. BALDEV RAJ and T. JAYAKUMAR, *ibid.* **8**(1-2) (1989) S126.
20. A. B. L. AGARWAL, J. R. FREDERICK and D. K. FELBECK, *Metall. Trans.* **1A** (1970) 1069.
21. B. CINA, *Acta Metall.* **6** (1958) 748.
22. PAT L. MANGONON Jr and GARETH THOMAS, *Metall. Trans.* **1** (1970) 1577.
23. DIETER FAHR, *ibid.* **2A** (1971) 1883.
24. BALDEV RAJ, Phd thesis, Indian Institute of Science, Bangalore, India (1989).
25. A. A. POLLOCK, *Non-Destruct. Test.* **6** (1973) 264.
26. K. V. KASIVISWANATHAN, V. VENUGOPAL, N. G. MURALIDHARAN and BALDEV RAJ, to be published.
27. Y. T. SUNG, D. I. LEE and Y. D. CHUANG, in "Third Pan Pacific Conference for Nondestructive Testing", Tokyo, Japan, 20–21 November 1980, pp. 165–74.

Received 23 October 1991
and accepted 24 March 1992